SANDIA REPORT

SAND
Unlimited Release
Printed September 2017

Molecule@MOF: A New Class of Opto-electronic Materials

A. Alec Talin, Viltalie Stavila, Mark D. Allendorf, Michael E. Foster, Yuping He, Francois Leonard, Catalin D. Spataru, Reese E. Jones

Prepared by
Sandia National Laboratories
Albuquerque, New Mexico 87185 and Livermore, California 94550

Sandia National Laboratories is a multimission laboratory managed and operated by National Technology and Engineering Solutions of Sandia, LLC, a wholly owned subsidiary of Honeywell International, Inc., for the U.S. Department of Energy's National Nuclear Security Administration under contract DE-NA0003525.

Issued by Sandia National Laboratories, operated for the United States Department of Energy by National Technology and Engineering Solutions of Sandia, LLC.

Available to DOE and DOE contractors from
U.S. Department of Energy
Office of Scientific and Technical Information
P.O. Box 62
Oak Ridge, TN 37831

Telephone: (865) 576-8401
Facsimile: (865) 576-5728
E-Mail: reports@osti.gov
Online ordering: http://www.osti.gov/scitech

Available to the public from
U.S. Department of Commerce
National Technical Information Service
5301 Shawnee Rd
Alexandria, VA 22312

Telephone: (800) 553-6847
Facsimile: (703) 605-6900
E-Mail: orders@ntis.gov
Online order: https://classic.ntis.gov/help/order-methods/

SAND2015-049
Printed September 2017
Unlimited Release

Molecule@MOF: A New Class of Opto-electronic Materials

A. Alec Talin, Viltalie Stavila, Mark D. Allendorf, Michael E. Foster, Yuping He, Francois Leonard, Catalin D. Spataru, Reese E. Jones
Materials Physics Department
Sandia National Laboratories
P. O. Box 969
Livermore, California 94551-MS9161

Patrick E. Hopkins
Department of Mechanical and Aerospace Engineering
University of Virginia
Charlottesville, Virginia 22904

Abstract

Metal organic frameworks (MOFs) are extended, nanoporous crystalline compounds consisting of metal ions interconnected by organic ligands. Their synthetic versatility suggest a disruptive class of opto-electronic materials with a high degree of electrical tunability and without the property-degrading disorder of organic conductors. In this project we determined the factors controlling charge and energy transport in MOFs and evaluated their potential for thermoelectric energy conversion. Two strategies for achieving electronic conductivity in MOFs were explored: 1) using redox active 'guest' molecules introduced into the pores to dope the framework via charge-transfer coupling (Guest@MOF), 2) metal organic graphene analogs (MOGs) with dispersive band structures arising from strong electronic overlap between the MOG metal ions and its coordinating linker groups. Inkjet deposition methods were developed to facilitate integration of the guest@MOF and MOG materials into practical devices.

TABLE OF CONTENTS

FIGURES

NOMENCLATURE

Abbreviation	Definition
Abbreviation	Definition
MOF	Metal organic framework
TCNQ	tetracyanoquinodimethane
MOG	Metal organic graphene anolog
BTC	Benzene tricarboxylic acid
VB, CB	Valence band, conduction band
PB	Prussian blue
HOMO	Highest occupied molecular orbital
LUMO	Lowest unoccupied molecular orbital
EPR	Electron paramagnetic resonance
XPS	X-ray photoelectron emission
TE	Thermoelectric
ZT	Thermoelectric figure of merit
TEG	Thermoelectric generator
PF	Power factor
PEDOT	poly(3,4-ethylenedioxythiophene)
CP	Coordination polymer
PDOS	Partial density of states

1. INTRODUCTION

Synthetically tunable optoelectronic materials are a long-standing, but elusive, technological goal. Inorganic semiconductors have outstanding properties, but limited synthetic flexibility; organic polymers offer chemical tunability and low-cost fabrication, but have poor mobility and long-term stability. Recently, we discovered that the electrical conductivity of a Metal-Organic Framework (MOF), a class of nanoporous, hybrid inorganic-organic crystalline solids, can be increased by >7 orders of magnitude by inserting redoxactive guest molecules in their pores (Molecule@MOF).[1] This conductivity is tunable by modifying the guest, guest loading, or MOF structure. Our experiments demonstrate that insulating, ohmic, and photoconducting behaviors are possible. MOFs possess long-range order and remarkable synthetic versatility, suggesting a new, disruptive class of opto-electronic materials is possible. The presence of metal ions with coordinating organic "linker" groups, coupled with rational design resulting from deep historical understanding of organometallic chemistry, enables an unprecedented degree of electrical tunability without the property-degrading disorder typical of organic conductors. With pore dimensions 1–10 nm, scaling conducting MOFs to dimensions approaching a single unit cell by bottom-up self-assembly is conceivable, avoiding fabrication issues that have stymied molecular electronics. The principle purpose of this research thrust is to determine the factors controlling charge and energy transport in MOFs and how can they be manipulated to create materials with unique and/or record performance. Achieving this goal will enable future generations of conducting MOF materials to be developed. New insight into the broader problem of conductivity in organics will also be gained, which still lacks scientific consensus.

MOFs are inorganic-organic hybrid polymers consisting of metal cations linked by organic groups such as carboxylates and amines, forming a crystalline, nanoporous structure. With record-setting surface areas (>7000 m^2/g), they are ideal for applications such as CO_2 sequestration and catalysis. While efforts to develop MOFs for these applications made major strides over the past decade, electrically conducting frameworks open up a host of other promising avenues, such as novel electronic devices, thermoelectrics, supercapacitors, electro-catalysts, and chemical sensors. Recently, we discovered a very large increase in conductivity induced in a well-known MOF by introducing a guest molecule into the MOF pores. The MOF is $Cu_3(BTC)_2$, and is composed of binuclear copper ions coordinated by benzene tricarboxylate (BTC) groups, forming a 'paddlewheel' like structure (a common motif in MOFs, see Fig. 1) and the guest molecule is TCNQ, a π-acid which forms charge-transfer complexes with a variety of organic and inorganic species. Extensive structural, spectroscopic and modeling analysis revealed that TCNQ binds strongly to the MOF when it bridges two neighboring copper paddlewheels, creating a continuous path through the MOF unit cell.[1] Furthermore, introduction of fluorinated and hydrogenated TCNQ derivatives such as F4-TCNQ and H4-TCNQ revealed that the conductivity can be 'tuned' by controlling the electronic coupling between the guest and the framework (Fig. 1d). Our discovery suggests that a completely new class of conducting electronic materials based on MOFs is possible that should enable a high degree of electrical tunability without the fabrication problems of molecular electronics or the molecular packing issues of bulk organic crystals.

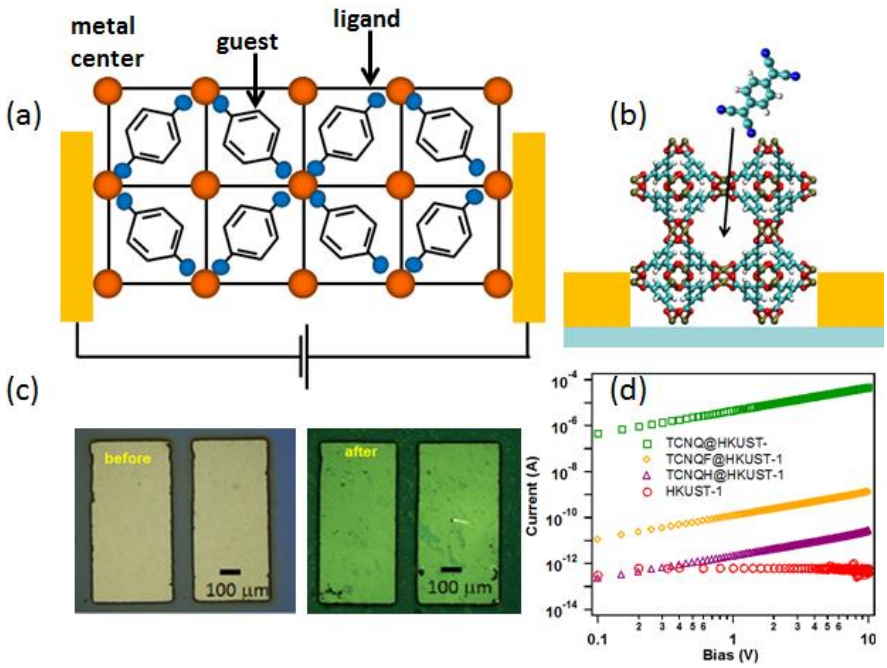

Figure 1. A generalized schematic for a guest@MOF electronic device b) TCNQ insertion into $Cu_3(BTC)_2$ pore c) $Cu_3(BTC)_2$ thin film deposited over Pt electrodes before (left) and after (right) TCNQ infiltration d) I-V curves before and after infiltration with TCNQ, F4-TCNQ, and H4-TCNQ

The goals of this LDRD include 1) develop fundamental understanding of the factors that lead to electronic conductivity in the TCNQ@$Cu_3(BTC)_2$ guest@MOF system; 2) explore potential application of TCNQ@$Cu_3(BTC)_2$ for thermoelectric energy conversion; 3) develop in house growth, characterize, and explore applications of the inherently conducting two-dimensional MOF system of $Ni_3(HITP)_2$ and related compounds.

. [BODY]

1.1. ELECTRONIC TRANSPORT IN METAL ORGANIC FRAMEWORKS

According to the band theory, solids can be classified as insulators, semiconductors, or metals based on the energy gap, E_g, separating the valence band (VB) from the conduction band (CB): $E_g > 4$ eV are insulators, $0 < E_g < 3$ eV are semiconductors, and $E_g < 0$ (i.e. partially filled band) are metals[2]. The band model works well for many solids in which strong electronic coupling between neighboring atoms leads to large band dispersion (i.e. large ΔE between bonding and antibonding orbitals), which makes it energetically favorable to delocalize carriers across many lattice sites. However, for many solids with less electronic coupling due to large difference in orbital energy between the bonding atoms and/or reduced orbital overlap typical of d-electron compounds, the classification based solely on bandgap can be misleading. For example, MnO and CrO have partially filled d-bands with an odd number of d-electrons, implying that irrespective of the ligand field splitting they should be metallic. Yet these, and many other transition metal oxides are insulators at room temperature due to the strong electrostatic repulsion that charge carriers experience when forced to doubly occupy a d-orbital in the process of moving across the lattice[3]. For solids with large band dispersion such as Si (see Fig. 2), the energy gained by delocalizing the

charge (~W/2) make the electron-electron repulsion effects insignificant. In metals, the screening effects are further reduced by electrostatic screening by the large density of free carriers. However, for materials with limited electronic coupling and narrow bandwidth, electron-electron repulsion becomes important, and in many transition metal compounds the CB splits into two sub-bands separated by the Hubbard energy, referred to as the lower and the upper Hubbard bands (LHB and UHB). Hubbard insulators can be turned into conductors by formation of anion or cation vacancies or by impurity doping. However, true metallic conduction (i.e. conductivity decreasing with increasing T) in many materials with bandwidth less than ~0.5 eV, is not observed even when the Fermi level moves into the VB or the CB due to strong carrier localization, i.e. the carriers are energetically trapped on lattice sites are require thermal agitation to hop from site to site. Prussian blue, composed of Fe^{2+} and Fe^{3+} ions coordinated by cyanide ligands, is an excellent example of a band insulator due to the ligand field splitting, but which should become metallic when oxidized to Berlin green or reduced to Prussian white. Nevertheless, oxidized or reduced PB exhibits thermally activated or hopping conduction due to formation of small polarons[4]. Small polarons form when the electrostatic energy gained in distorting the lattice by the charge carrier exceeds the energy gained by carrier delocalization (i.e. the bandwidth) leading to carrier trapping at individual lattice sites. Typical polaron mobilities are <<1 cm^2/Vs, compared to >100 cm^2/Vs measured for elemental and compound semiconductors.

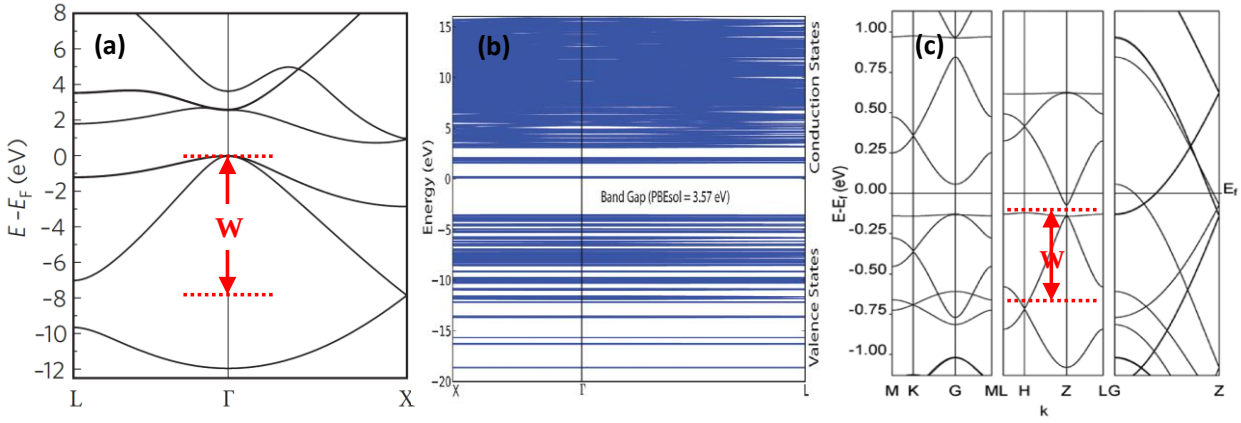

Figure 2. Calculated band diagrams. (a) Si. Adapted from ref. 9. Copyright 2011 Springer. (b) MOF-5. Reproduced with permission from ref. 10. (c) $Ni_3(HITP)_2$. Reproduced with permission from ref. 14. Copyright 2016 American Chemical Society. The bandwidth (W) is approximately 8 eV, 0 eV, and 0.8 eV, respectively.

With low atomic density and the strong localization of the electron wave function characteristic of many metal-oxygen bonds, most MOFs are expected to have little or no band dispersion and behave as insulators, as is the case of MOF-5 (see Fig. 2b)[5]. Of the approximately 20 conducting porous frameworks discovered to date,[6] only about half report on thermal dependence of the conductivity, and of these the majority have activation energies in the range of several hundred meVs, consistent with formation of small polarons[6]. The process of charge hopping between neighboring sites can be described using a configuration coordinate diagram with the x-axis representing the distortion coordinate around the site with the trapped carrier [7, 8]. As discussed later for TCNQ@$Cu_3(BTC)_2$ Guest@MOF compound, the activation barrier for charge hopping from one site to the next depends on the degree of electronic coupling between the centers:

strong coupling leads to large degree of charge delocalization, analogous to Class III type compounds in the Robin and Day nomenclature, while no coupling corresponds to Class I type compound with complete charge localization. Like Prussian blue, most conducting MOFs to date appear to fall into the Class II category, for which the electronic coupling between the two sites is sufficiently large so that only a small amount of energy is necessary for charge transfer.

A notable exception to the hopping type transport observed to date in most conducting MOF and Guest@MOF materials is the framework $Ni_3(HITP)_2$, consisting of π-stacked 2D sheets of HITP (HITP≡2,3,6,7,10,11-hexaaminotriphenylene) ligands coordinated to Ni^{2+} ions. $Ni_3(HITP)_2$ and other metal-organic graphene analogues (MOGs), assembled from multitopic dithiolene and o-semiquinone aromatic organic moieties bridged by square-planar metal ions, have high degree of in-plane charge delocalization, similar to that observed in graphene and layered metal chalcogenites[9]. However, unlike the inorganic 2D conductors, which do not easily lend themselves to chemical functionalization, the electronic and optical properties of MOFs and MOGs can be tuned by chemically altering the linker, metal ion, or by introducing guest molecules into the pores. When first reported by Dinca et al. the observed conductivity versus temperature characteristic for $Ni_3(HITP)_2$ did exhibit hopping type transport, though with a very low activation energy of ~0.025 eV, estimated based on the conductivity versus T data[10], and consistent with the relatively narrow bandwidth of ~0.5 eV estimated from the dispersion relation calculated for $Ni_3(HITP)_2$ (Fig. 2c). More recently, however, Xu et al. reported hole mobilities of ~40 cm^2/Vs in field effect transistor (FET) type structures with smooth $Ni_3(HITP)_2$ layers ~100 nm thick deposited over Si/SiO_2 substrates[11]. This relatively large value exceeds the values for most single crystalline organic conductors and suggests a high degree of carrier delocalization.

1.2. DONOR-BRIDGE-ACCEPTOR MODEL FOR CONDUCTIVITY IN $Cu_3(BTC)_2$

One way to understand the origin of conductivity in $TCNQ@Cu_3(BTC)_2$ is to consider the donor −bridge− acceptor (DBA) model.26 In this model, TCNQ molecules are coordinated in a bridging geometry through C≡N groups in the 7 and 8 positions to two copper paddlewheel SBUs in the $Cu_3(BTC)_2$ pore (Figure 3, left). This system is similar to the symmetric molecular mixed valence molecules that undergo inner-sphere electron transfer via ditopic bridging ligands, and to the ruthenium-acetate coordination polymers and the well-known Prussian blue semiconductor[12]. In our model, the electronic coupling between the donor (A) and acceptor (B) diabatic states (dashed red lines) yields an adiabatic ground state X and excited states A1 and A2 (solid blue lines). This interaction is quantified by the electronic coupling matric element H_{AB} between the donor and acceptor and by the matrix elements $H_{AC} = H_{BC}$ between the donor or acceptor and the bridge. As discussed by Brunschwig et al. and others, charge transfer can occur by either a super exchange mechanism, involving mixing between electronic excited states and the ground state, or by the so-called "chemical mechanism," in which the bridge is an intermediate that is oxidized or reduced during the reaction.[8] The super exchange mechanism generates new charge transfer features in the absorption spectrum (indicated by the vertical arrows in Figure 3), which is consistent with the strong new absorption bands that appear upon infiltration of $Cu_3(BTC)_2$ with TCNQ[1]. $TCNQ@Cu_3(BTC)_2$ is not a mixed-valence system, however, as shown by XPS measurements. Therefore, some other aspect of the electronic structure must be responsible for creation of charge carriers in this system. We can rule out the chemical mechanism on both theoretical and experimental grounds. In the simplest three-state model case, the mediating bridging state is located above the intersection of the crossing of the donor and acceptor diabatic states. If direct coupling between the donor and acceptor diabatic states is zero ($H_{AB} = 0$) and the

donor-bridge coupling matrix elements are equal (symmetric system, so $H_{AC} = H_{BC}$), the system becomes analogous to a two-state model. However, this approximation is not valid if the donor-bridge electronic coupling is large or the bridging state minimum lies below the intersection of the donor and acceptor diabatic curves. In the latter case, theory predicts that a third minimum may form between those of the donor and acceptor predicted by two-state models that, if sufficiently stable, could create an intermediate in the electron transfer process.

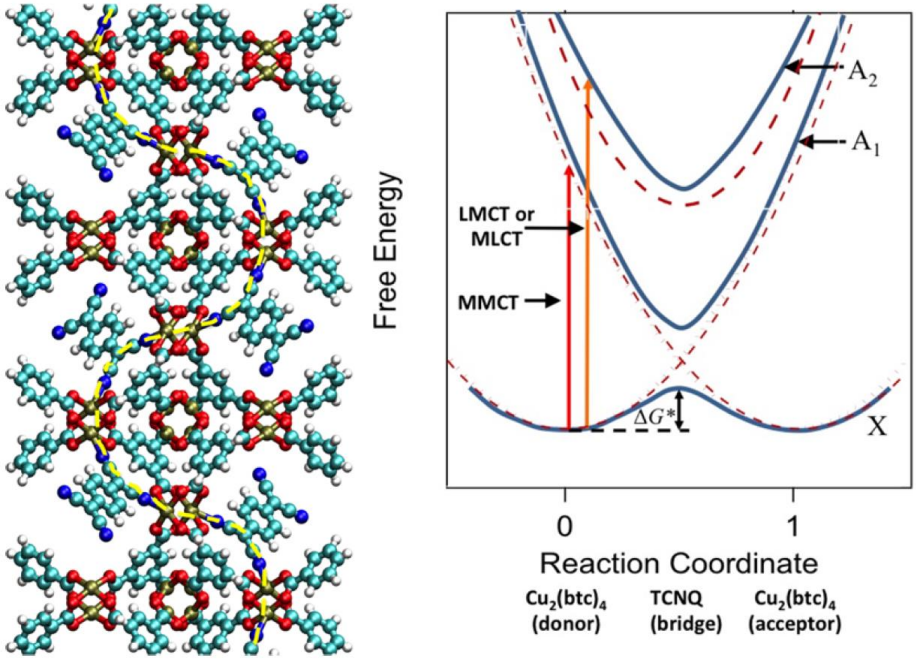

Figure 3. Proposed DBA structure of TCNQ@$Cu_3(BTC)_2$. Adapted from ref 1. Dashed line indicates the pathway for charge conduction. Right: Energy vs reaction coordinate for a three-state DBA system. Solid blue lines indicate the adiabatic states, which are the result of mixing among the diabatic states (dashed red lines). Adapted from ref 8.

This model is conceivable for TCNQ@ $Cu_3(BTC)_2$, as seen in Figure 13, where it is shown that the LUMO of TCNQ falls within the $Cu_3(BTC)_2$ HOMO−LUMOgap, and calculations of H_{AC} computed for a representative molecular cluster analogue (UHF/VTZP level of theory using the broken-symmetry approach and charge constraints26) is of similar magnitude to the energy difference between the TCNQ LUMO and the $Cu_3(BTC)_2$ HOMO. The predicted coupling is large, which we attribute to the high degree of orbital overlap between TCNQ and the Cu d(z2) orbital. Experimental evidence from EPR and XPS also does not support the formation of such an intermediate. Modifying the extent of electronic coupling by replacing TCNQ with either the fluorinated analogue (F4-TCNQ) or the version in with the ring fully hydrogenated (H4-TCNQ), results in conductivity changes (Figure 10) and reduction of the H_{AC} values (Figure 3) consistent with the superexchange model. Specifically, fluorinating the ring yields similar energy levels to TCNQ but decreased H_{AC}, yielding reduced (but not negligible) conductivity. In contrast, fully hydrogenating the ring removes the aromatic character and drastically reduces H_{AC}, leading to

conductivity only slightly above those of uninfiltrated $Cu_3(BTC)_2$. Whereas the DBA model suggests a local microscopic mechanism for charge transport, for electrical conductivity to emerge over mesoscopic to macroscopic dimensions, a long-range organization of the DBA sites is necessary. The proposed structure shown in Figure 3 can enable such long-range charge transport in TCNQ@MOF. In this case, the presence of one TCNQ molecule per pore allows the formation of a continuous chain through the MOF crystal. Experimental evidence for this organization comes from measurements of the conductivity as a function of infiltration time, where we find a dependence reminiscent of percolative transport.[1] The forgoing analysis does not specify the identity of the charge carriers (electrons or holes) or the nature of the transition state corresponding to the low activation barrier for conductivity. The sign of the Seebeck coefficient (which we discuss in the next section) provides an unambiguous determination of the charge carrier; measurements we performed indicate that these are holes in TCNQ@$Cu_3(BTC)_2$ films. Because $Cu_3(BTC)_2$ is already fully oxidized, the remaining questions are, what is the origin of these holes and how is their formation related to the thermal activation process? We hypothesize that the answer lies in the antiferromagnetic super exchange coupling of the unpaired Cu(II) d electrons in the SBU. As discussed above, this produces a singlet ground state with a triplet located 340 cm^{-1} (0.042 eV) above it. This splitting is nearly identical to the activation energy measured for the electronic conductivity, suggesting that holes on the Cu(II) ions are generated by thermally populating the triplet state, in which the $d_{(x2-y2)}$ electrons are magnetically uncoupled. Given a population of holes, Marcus charge transfer theory in solution indicates that the transition state corresponds to a reorganization of solvent molecules and that this occurs prior to the actual movement of charge. In Guest@MOF systems, it is unclear whether solvent molecules coexisting in the pores with the guest are available to stabilize the charge. Marcus theory has also been extended to conjugated molecular wires, where the transition state for thermally activated hopping transport is thought to be reached by vibrational and torsional reorientations of the molecule.[13] In TCNQ@$Cu_3(BTC)_2$, this reorientation would presumably be due primarily to twisting or vibrations of the TCNQ molecule.

2. METAL ORGANIC FRAMEWORKS FOR THERMOELECTRIC ENERGY CONVERSION APPLICATIONS

Motivated by low cost, low toxicity, mechanical flexibility, and conformability over complex shapes, organic semiconductors are currently being actively investigated as thermoelectric (TE) materials to replace the costly, brittle, and non-eco-friendly inorganic TEs for near ambient temperature applications. Metal organic frameworks (MOFs) share many of the attractive features of all-organic polymers, including solution processability and low thermal conductivity. A potential advantage of MOFs and Guest@MOF materials is their synthetic and structural versatility, which allows both the electronic and geometric structure to be tuned through the choice of metal, ligand, and guest molecules which could solve the long-standing challenge of finding stable, high ZT n-type organic semiconductors, as well as promote high charge mobility as a result of the long-range crystalline order inherent in these materials. In this article we review the recent advances in the synthesis of MOF and Guest@MOF TEs and discuss how the Seebeck coefficient, electrical conductivity and the thermal conductivity could be tuned to further optimize their TE performance.

2.1. INTRODUCTION TO THERMOELECTRICS

When two parts of an electric conductor are held at different temperatures, charge carriers diffuse from the hot to the cold regions, producing a voltage difference that is the basis for the thermoelectric (TE) Seebeck effect. The Seebeck coefficient, *S,* is the voltage difference resulting from a temperature gradient and a measure of thermopower. It can be positive (for hole conductors) or negative (for electron conductors) and ranges from a few μV/K typically measured for metals, to values well over 1000 μV/K that can be observed in lightly doped semiconductors[14]. A TE generator (TEG) is a solid state device that takes advantage of the Seebeck effect to directly convert a temperature gradient into electric work.

The efficiency of a TE conversion device is determined by the figure of merit of the materials comprising the device:

$$ZT = \frac{S^2 \sigma T}{\kappa} \qquad (1)$$

where σ is the electrical conductivity, T is the average temperature, κ is the thermal conductivity, and $S^2\sigma$ (W/mK^2) is the power factor (*PF*) of the material. Materials which combine high values of S and σ/κ are therefore attractive for TE applications. There is no theoretical limit on the value of *ZT*; however, finding materials with *ZT* significantly greater than 1 is challenging due to the interdependencies that exist among the parameters.

A large S requires that σ (or electronic density of states) near the Fermi level E_F changes rapidly[15], as indicated by the Mott expression for S,

$$S = \frac{\pi^2}{3}\frac{\kappa_B}{q}\kappa_B T\left\{\frac{d\left[\ln(\sigma(E))\right]}{dE}\right\}_{E=E_F} \qquad (2)$$

where κ_B is the Boltzmann constant, q is the elementary charge. Materials such as lightly doped semiconductors for which $n(E)_{E=E_F}$ (or $p(E)_{E=E_F}$) changes rapidly with energy are expected to have large S values; however, such materials also tend to be poor electrical conductors since the free carrier concentration is low, and therefore the *ZT* factor is low. A compromise between

maximizing S and σ favors low bandgap semiconductors (*doping*~10^{19}-10^{21}/cm^3) such as Bi_2Te_3 and its alloys.

Designing materials with optimum *ZT* is further complicated by the relationship between κ and σ. κ is the sum of lattice thermal conductivity, κ_l, and the electronic thermal conductivity, κ_e. According to the Wiedemann-Franz law, $\kappa_e / \sigma = LT$ where the Lorenz number L=2.4×10^{-8} $J^2K^{-2}C^{-2}$ for a free electron metal. For semiconductors with relatively low free carrier concentration (<10^{19}/cm^3), κ is dominated by the lattice contribution. However, as electronic carrier concentration and mobility increase, so does κ_e, including in the case of conducting polymers such as poly(3,4-ethylenedioxythiophene) (PEDOT), as was recently demonstrated by Weathers et al.[16] and Liu et al.[17] Hence, another major thrust in TE material engineering is minimizing the lattice contribution to achieve the lowest possible total κ with a maximal *PF*.

2.2. THERMOELECTRIC MATERIALS

Inorganic semiconductors such as Bi_2Te_3 and some of its alloys with Sb and Sn have adequate efficiency for a variety of niche applications[18],[19] but have not been widely adopted because they are difficult to deposit over complex and/or high surface area structures, are not eco-friendly, and are too expensive for many applications. Nanostructuring and superlattices have yielded structures with *ZT*>2, but these complex materials still remain impractical and too expensive for widespread applications such as integration with solar cells or for powering wearable electronics/sensors powered by body heat.[20]

As an alternative to inorganic materials, conducting polymers have recently attracted much attention for TE applications, motivated by their low material cost, ease of processability, non-toxicity, mechanical flexibility and low thermal conductivity.[21] Conducting polymers such as polyacetylene, polyaniline, polypyrrole, and poly(3,4-ethylenedioxythiophene) (PEDOT) consist of long, conjugated molecular chains with varying degree of crystallinity.[22] In virtually all cases, significant σ in polymers requires doping. The dopants are typically organic or inorganic acids that remove electrons from the valence band of the polymers, but are themselves insulators that can occupy significant volume fraction, as well as cause structural disorder, decrease chain-to-chain electronic coupling, and depress carrier mobility.[23] Minimizing the dopant volume and precise control of oxidation state recently led to PEDOT:PSS with a *PF* of 480 $\mu Wm^{-1}K^{-2}$.[24] This result was recently questioned because σ and κ were not measured for the same specimens, or in the same direction with respect to the specimen geometry.[16]

Practical TEGs require both p- and n-type elements. Unfortunately, achieving chemically stable n-type conducting polymers is challenging because the position of the lowest unoccupied molecular orbital (LUMO) level relative to vacuum level, the electron affinity (*EA*), is low for most linear chain conjugated organic polymers.[25] Recently, electron deficient conjugated systems with *EA* below -4.0 eV have emerged, but the best performing among these, BDPPV doped with N-DMBI N-((4-(1,3-dimethyl-2,3-dihydro-1H-benzoimidazol-2-yl)phenyl)dimethylamine), yielded a *PF* of 0.28×10^{-4} $Wm^{-1}K^{-2}$, well below the values achieved for p-type polymers.

An alternative approach to is to consider coordination polymers (CPs) (MOFs are a subset of CPs with permanent porosity), which are composed of repeating units of metal-organic coordination complexes. Unlike all-organic conjugated polymers for which the valence and conduction bands are associated with the delocalized π and π^* orbitals of the carbon backbone,

respectively, the electronic structure of CPs is dominated by the transition metal d electrons and their interaction with the organic ligands.[4],[26] In fact, the CP poly[K_x(Ni-ett)], composed of Ni(II) ions coordinated to 1,1,2,2-ethenetetrathiolate (ett) currently holds the record as the n-type polymer with the highest *ZT* at room temperature. Unfortunately, a solution-based processing route to poly[K_x(Ni-ett)] has not yet been demonstrated.

2.3. CONDUCTING METAL-ORGANIC FRAMEWORK THERMOELECTRICS

MOFs share many of the advantages of all-organic polymers TEs for applications requiring large area processable, non-toxic, and low-cost materials. Additionally, MOFs and Guest@MOF materials offer higher thermal stability (up to ~400^{o}C in some cases) and have long-range crystalline order, which could be harnessed to improve charge mobility. MOFs offer tremendous synthetic and structural versatility for optimizing the electronic structure for high p- and n-type *ZT* through choices of metal and ligand. The long-range crystalline order of MOFs could promote high charge mobility to increase σ without adversely affecting *S*. A further aspect that differentiates MOFs from the broader class of non-porous CPs is their ability to adsorb a large variety of molecules and nanostructures within their pores to further tune or dramatically change the material's electronic and thermal transport characteristics (see the article by Fischer and Allendorf in this issue). The field of MOF-based TEs is still in its infancy, however, and to date only one MOF has been explored for TE applications: the TCNQ@$Cu_3(BTC)_2$ guest@MOF system.

2.3.1. TCNQ@$Cu_3(BTC)_2$ thermoelectric

The $Cu_3(BTC)_2$ MOF forms face centered cubic crystals consisting of Cu(II) dimers coordinated by four BTC (benzene 1,3,5-tricarboxylate) linkers (Fig. 1B). The $Cu_3(BTC)_2$ MOF can be deposited by a variety of methods including solution-based thin film growth and ink jet printing.[1, 27] Ink jet printing is particularly attractive for low cost TE fabrication since relatively thick layers with desired pattern and current collectors can be rapidly deposited on low-cost substrates, as shown in ref. 18 and our laboratory (Fig. 1c).

When $Cu_3(BTC)_2$is infiltrated with tetracyanoquinodimethane (TCNQ), the Cu(II) dimers become bridged by TCNQ molecules, forming an electronic conduction pathway and increasing σ from $<10^{-9}$ S/m to ~0.1 S/m.[1] When a thin film of TCNQ@$Cu_3(BTC)_2$ on is placed onto a stage with a thermal gradient, a positive voltage is measured between the cold and hot sides (see Fig. 2a, b) with *S*~400 μV/K at room temperature (Fig. 2c, d), indicating that holes are the dominant electronic charge carriers in the infiltrated framework.

The positive *S* is consistent with the calculated density of states which shows how E_F in $Cu_3(BTC)_2$ moves from the mid-gap to the valence band upon infiltration with TCNQ (Fig. 1c,d). This can be rationalized by the fact that the LUMO levels of TCNQ lie very close to the $Cu_3(BTC)_2$ valence band due to the large electron affinity of TCNQ. The blue line in the figure indicates that the TCNQ LUMO levels are situated just above E_F, whereas the $Cu_3(BTC)_2$ valence band is located just below E_F. Despite the large *S*, the relatively low σ results in a comparatively low *PF* of ~0.06 μW/mK^2 (see Table I for comparison).

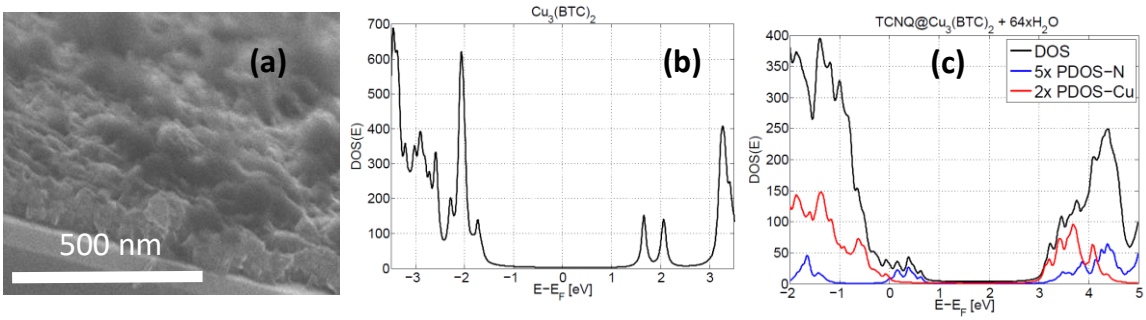

Figure 4.(a) Scanning electron microscope image of $Cu_3(BTC)_2$ deposited using liquid phase layer by layer growth (left) and an optical image of $Cu_3(BTC)_2$ (blue line) with Ag electrodes all deposited on paper by ink jet printing (right). (b) Electronic density of states calculated *ab initio* -- for $Cu_3(BTC)_2$ E_F is in the electronic gap. c) For TCNQ@$Cu_3(BTC)_2$ E_F is near the MOF valence band. The blue lines indicate the partial density of states (PDOS) obtained by projecting the wavefunctions on the TCNQ N atoms, while the red lines indicate the PDOS obtained by a similar projection on the MOF Cu atoms. Reprinted with permission from ref. 45, © 2015 Wiley.

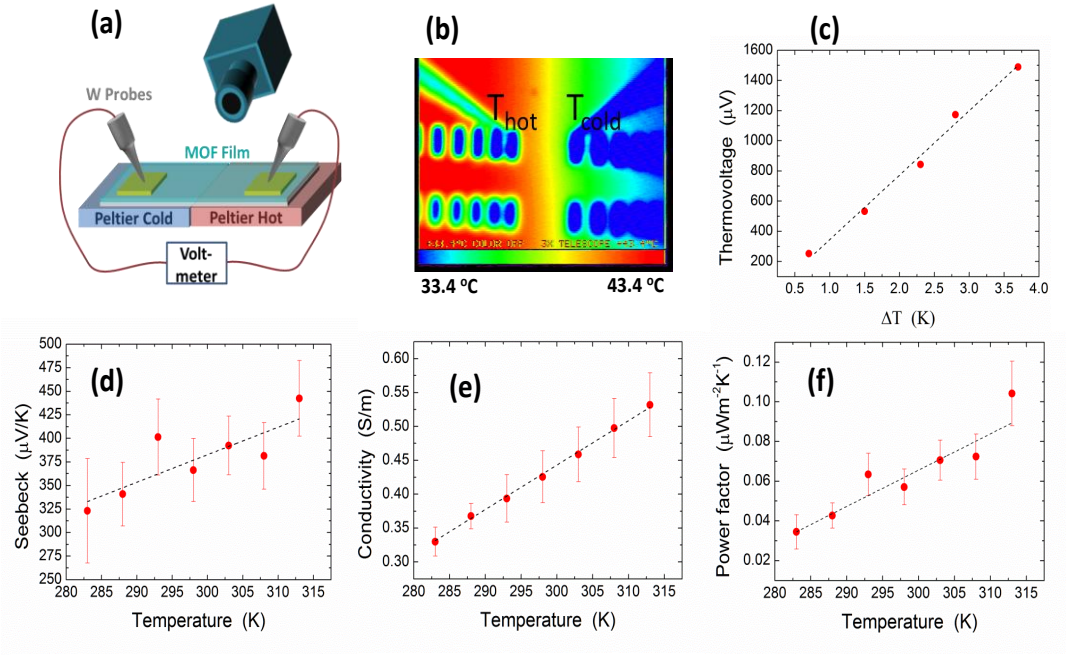

Figure 5. TE characterization of the MOF thin film devices. a) Two Peltier coolers are used to heat and cool the two sides of the substrate and an IR camera is used to measure the T profile. b) IR image taken during one of the measurements. The electrical contacts appear cold in the image because of their different emissivity compared with the MOF. c) Measured voltage as a function of ΔT. S is extracted from the linear fit. d) S as a function of T. The dashed line is a linear fit. e) σ as a function of T. The dashed line is a linear fit that could represent a thermally activated process with activation energy of 50 meV. f) PF as a function of T. The dashed line is a linear fit. Reprinted with permission from ref. 45, © 2015 Wiley.

To determine the *ZT*, κ for TCNQ@$Cu_3(BTC)_2$ was measured using time domain thermoreflectance (TDTR) yielding a room-temperature value of 0.27 ± 0.04 $Wm^{-1}K^{-1}$. This κ is comparable to the best thermoelectric polymers and an order of magnitude smaller than Bi_2Te_3. To understand the factors that dominate this low thermal conductivity, we used molecular dynamics simulations to calculate the κ_l of crystalline $Cu_3(BTC)_2$ and TCNQ@$Cu_3(BTC)_2$ obtaining a κ_l of 0.58 $Wm^{-1}K^{-1}$ for the un-infiltrated crystalline MOF and 3.84±0.27 $Wm^{-1}K^{-1}$ for the infiltrated crystalline MOF. The addition of TCNQ significantly increases κ_l, which is, at least in part, due to the increased density of phonons in the low-frequency/high group-velocity range. Since the calculated values simulate a single crystal rather than a polycrystalline material, the difference with the experimental values indicates other significant aspects of phonon transport in this MOF are not captured in our MD simulations.

Inserting the experimental values we measured for *S*, σ (=0.45 S/m), and κ in Equation 1, we obtain $ZT \approx 7\times10^{-5}$ at 298 K, a value well below those of the best inorganic thermoelectric materials (see Table I). While the MOF *S* is more than five times larger than PDOT:PSS and κ_l is comparable, it is clear that the TCNQ@$Cu_3(BTC)_2$ σ is the main reason for the reduced performance. Improving crystallinity will likely increase σ, but may also increase κ.

2.4. THERMAL TRANSPORT IN METAL ORGANIC FRAMEWORKS

A maximum ratio of s/κ is a goal in designing an ideal TE material, giving rise to the well-known quest for a phonon-glass/electron-crystal.[28] The quest to synthesize solids with ultralow κ_l has focused on disordered or amorphous phases where structural periodicity and thus phonons, are absent.[29] In this case, the length scales of vibrational energy exchange that contribute to the thermal conductivity can be on the order of the atomic spacing,[30-32] akin to Einstein's original theory of how energy moves through solids.[33, 34] However, introducing disorder in the atomic structure may also have detrimental effects on σ. Therefore, maintaining crystallinity while reducing κ_l via limiting the length scales of vibrational energy transfer and other means is a more viable path to achieving maximal material *ZT*.

In the context of the widely-adopted kinetic theory, $\kappa_l = 1/3\ \Sigma_m\ (cv\ell)_m$, where *c* is the heat carried per mode *m*, *v* is the speed of propagation, ℓ and the mean free path of the carrier, we know that low κ_l result from weak bonding, high atomic mass, complex atomic structures, and high anharmonicity, each of which systematically decreases the quantities *c*, v and ℓ via different nanoscale mechanisms. MOFs are composed of a variety of atomic species with different masses and heterogeneous bonds. This heterogeneity in masses and bond stiffness directly affects ℓ for any given phonon mode, leading to low κ_l. Huang et al. calculated that the intrinsic κ_l of MOF-5 is 0.3 $Wm^{-1}K^{-1}$ [35] resulting from a characteristic ℓ =0.83 nm that is considerably smaller than the lattice constant of 2.6 nm, and relatively independent of temperature. Also Wang et al. used first principles to determine that due to its large and complex unit cell, MOF-74 has a large population of optical phonons that lead to over 50% of the energy being carried by phonons with ℓ <2 nm.[36]

The open, mechanically soft structure of MOFs leads to relatively low energy propagation velocities.[35] Huang et al. calculated an atomic density of 24.6 atoms/nm^3 and a sound speed of

1184 m/s for MOF-5.[35] The open structure and large porosity ratios in MOFs lead to strong scattering of all phonons at moderate temperatures, resembling the phonon-glass concept, and a heat capacity below the Dulong-Petit limit .[37] However, it is important to note that increasing the porosity of a MOF will likely have detrimental effects on electrical conductivity and hence *ZT*.

The introduction of guest molecules into MOFs can have a variety of effects on κ_l. Weakly interacting, light molecules such as infiltrated water will likely have no significant effect unless they are in abundance; however, heavier, loosely bound rattling atoms in the MOF pores can significantly reduce κ_l, as has been previously observed for zeolites, skutterudites, and clathrates.[38-43] In particular, rattlers reduce κ_l due to the creation of localized modes, enhancement of anharmonicity and reduction of group velocities.[43] Indeed, acoustic phonons in MOFs have been described to exhibit "rattling-like behavior", which results in exceptionally high anharmonicity of these modes.[43] This implies that the acoustic modes in MOFs could be close to the situation where phonons are "equally strongly damped", as in amorphous and disordered materials.[37, 43]

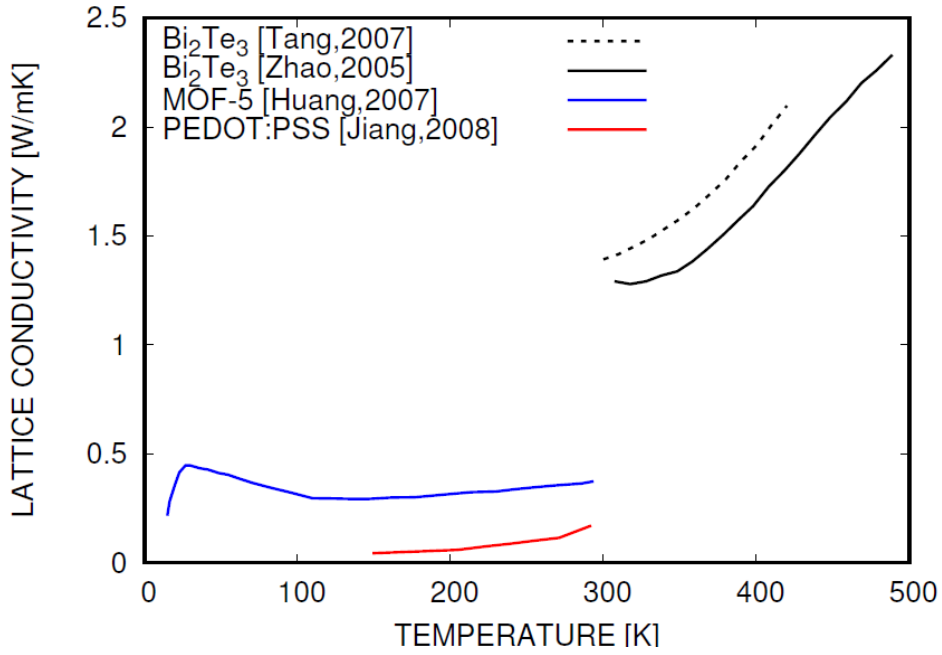

Figure 6. κ_l as a function of T for several materials

Furthermore, while the use of infiltration to achieve the guest@MOF can lead to bond stiffening, the resulting variable and complex bonding environments could, in principle, be tuned to enhance vibrational scattering and reduce ℓ. An increase in bond heterogeneity could increase the "rattling-like" behavior of the acoustic modes, increasing anharmonicity and decreasing thermal transport of the affected modes.[44] The infiltration approach could potentially be engineered to create further reductions in the heat carrying phonons, while providing significant improvement to σ, as discussed.

The temperature dependence of κ_l is also of interest for TE applications given that ΔT between the hot and cold sides may be >100 K. Ordinarily, in defect-free materials above their Debye temperature, κ_l is dominated by Umklapp scattering which leads to a T^{-1} scaling. However, experimentally measured κ's of typical semiconducting organic materials, Bi_2Te_3 and MOF-5 exhibit only slightly increasing trends, similar to glassy/amorphous materials as shown in Fig.3. [17, 45-50]

2.5. CONCLUSIONS

The need for low-cost, mechanically flexible, and environmentally friendly TE energy conversion devices has led to increased attention to organic and hybrid organic-inorganic TE materials. Despite impressive progress, substantial challenges remain to increase charge mobility due to inherent and dopant-induced structural disorder, as well as the scarcity of n-type organic conductors. In this article, we have argued that electrically conducting MOFs could solve the disorder problem common to polymers, providing within a single material the highly ordered structure of inorganic conductors with the tunable properties and low cost of organics. Furthermore, we have used the example of TCNQ@$Cu_3(BTC)_2$ framework to illustrate how structure-inherent nanoscale porosity of MOFs provides a route to tuning the electronic properties of these materials with guest molecules without increasing structural disorder. Although σ of TCNQ@$Cu_3(BTC)_2$ is still too low to make it an attractive TE, the recent emergence of several inherently conducting, porous frameworks whose electronic and thermal transport properties could be further tuned using guest molecule infiltration, makes MOFs and Guest@MOFs promising for further exploration for TE energy conversion applications.

3. MOLECULE@MOF PUBLICATIONS

1. L. Sun, B. Liao, D. Sheberla, D. Kraemer, J. Zhou, E. A. Stach, D. Zakharov, V. Stavila, A. A. Talin, M. D. Allendorf, G. Chen, F. Léonard, M. Dincă, "A Microporous and Naturally Nanostructured Thermoelectric Metal-Organic Framework with Ultralow Thermal Conductivity", *Joule*, accepted

2. J. Chae, S. An, G. Ramer, V. Stavila, G. Holland, Y. Yoon, A A. Talin, M. D. Allendorf, V. Aksyuk, A. Centrone, "Nanophotonic AFM Transducers Enable Chemical Composition and Thermal Conductivity Measurements at the Nanoscale", *Nano Lett.* DOI: 10.1021/acs.nanolett.7b02404

3. Y. He, C. D. Spataru, F. Leonard, R. E. Jones, M. E. Foster, M. D. Allendorf, A. A. Talin Two-dimensional metal–organic frameworks with high thermoelectric efficiency through metal ion selection", *Phys.Chem.Chem.Phys*., 19, 19461, (2017).

4. I. Stassen, N. Burtch, A. A. Talin, P. Falcaro, M. D. Allendorf, R. Ameloot, "An updated roadmap for the integration of metal-organic frameworks with electronic devices and chemical sensors", *Chem. Soc. Rev*. 46, 3185 (2017).

5. A. A. Talin, R. E. Jones, P. E. Hopkins, "Metal Organic Frameworks for Thermoelectric Energy Conversion Applications", *MRS Bulletin* 41, 877, (2016).

6. M. D. Allendorf, R. Medishetty, R. A Fischer, Guest molecules as a design element for metal-organic frameworks. MRS Bulletin, 41, 865 (2016)

7. M. E. Foster, K. Sohlberg, C. D. Spataru, M. D. Allendorf, Proposed Modification of the Graphene Analogue Ni-3(HITP)(2) To Yield a Semiconducting Material. *Journal of Physical Chemistry C, 120*, 15001 (2016)

8. A. M. Ullman, J. W. Brown, M. Foster, F. Leonard, K. Leong, V. Stavila, M. D. Allendorf, Transforming MOFs for Energy Applications Using the Guest@MOF Concept. *Inorganic Chemistry 55*, 7233 (2016).

9. M. D. Allendorf, A framework for success. *Nature Energy* 1 (2016).

10. M. D. Allendorf, V. Stavila, NANOPOROUS FILMS From conventional to conformal. Nature Materials 15, 255 (2016)

11. K. J. Erickson, F. Léonard, V. Stavila, M. E. Foster, C. D. Spataru, R. E. Jones, B. M. Foley, P. E. Hopkins, M. D. Allendorf, and A. A. Talin, "Thin Film Thermoelectric Metal–Organic Framework with High Seebeck Coefficient and Low Thermal Conductivity", *Adv. Mat.* 27, 3453 (2015).

12. (Cover) M. D. Allendorf, M. E. Foster, F. Léonard, V. Stavila, P. L. Feng, F. P. Doty, K. Leong, E. Yue Ma, S. R. Johnston, and A. A. Talin, "Guest-Induced Emergent Properties in Metal−Organic Frameworks" *J. Phys. Chem. Lett.* 6, 1182 (2015).

4. MOLECULE@MOF INTELLECTUAL PROPERTY

1. 1. 9,347,923 “Colorometric detection of water using MOF-polymer films and composites”, Allendorf; M. D., Talin; A. A.
2. 2. 9,428,525 “Tunable electrical conductivity in metal-organic framework thin film devices” Talin; A. A., Allendorf; M. D., Stavila; V., Leonard; F.
3. 3. 9,546,887 “Multiaxis sensing using metal organic frameworks” Talin; A. A., Allendorf; M. D., Leonard; F., Stavila; V.

REFERENCES

[1] A.A. Talin, A. Centrone, A.C. Ford, M.E. Foster, V. Stavila, P. Haney, R.A. Kinney, V. Szalai, F. El Gabaly, H.P. Yoon, F. Leonard, M.D. Allendorf, Tunable Electrical Conductivity in Metal-Organic Framework Thin-Film Devices, Sci. 343(6166) 66-69. (2014).

[2] R.E. Hummel, Electronic Properties of Materials, Fourth Edition, 2011.

[3] Y. Zhou, S. Ramanathan, Mott Memory and Neuromorphic Devices, Proceedings of the IEEE 103(8), 1289-1310, (2015).

[4] M. Pajerowski Daniel, T. Watanabe, T. Yamamoto, Y. Einaga, Electronic conductivity in Berlin green and Prussian blue, Physical Review B - Condensed Matter and Materials Physics 83(15) (2011).

[5] C.H. Hendon, D. Tiana, A. Walsh, Conductive metal-organic frameworks and networks: fact or fantasy?, Phys. Chem. Chem. Phys. 14(38) 13120-13132, (2012).

[6] L. Sun Lei, M.G. Campbell, M. Dinca, Electrically Conductive Porous Metal-Organic Frameworks, Angewandte Chemie International Edition 55(11) 3566-79, (2016).

[7] P.A. Cox, The electronic structure of transition metal oxides and chalcogenides, in: C. Schlenker, J. Dumas, M. Greenblatt, S. vanSmaalen (Eds.), Physics and Chemistry of Low-Dimensional Inorganic Conductors, Plenum Press Div Plenum Publishing Corp, New York, pp. 255-270, 1996.

[8] B.S. Brunschwig, C. Creutz, N. Sutin, Optical transitions of symmetrical mixed-valence systems in the Class II-III transition regime, Chemical Society Reviews 31(3) 168-184, (2002).

[9] A.M. Ullman, J.W. Brown, M.E. Foster, F. Leonard, K. Leong, V. Stavila, M.D. Allendorf, Transforming MOFs for Energy Applications Using the Guest@MOF Concept, Inorganic Chemistry 55(15) 7233-7249, (2016).

[10] D. Sheberla, L. Sun, M.A. Blood-Forsythe, S. Er, C.R. Wade, C.K. Brozek, A. Aspuru-Guzik, M. Dinca, High Electrical Conductivity in Ni-3(2,3,6,7,10,11-hexaiminotriphenylene)(2), a Semiconducting Metal-Organic Graphene Analogue, Journal of the American Chemical Society 136(25) 8859-8862, (2014).

[11] G. Wu, J. Huang, Y. Zang, J. He, G. Xu, Porous Field-Effect Transistors Based on a Semiconductive Metal–Organic Framework, Journal of the American Chemical Society (2016).

[12] H. Miyasaka, N. Motokawa, S. Matsunaga, M. Yamashita, K. Sugimoto, T. Mori, N. Toyota, K.R. Dunbar, Control of Charge Transfer in a Series of Ru-2(II,II)/TCNQ Two-Dimensional Networks by Tuning the Electron Affinity of TCNQ Units: A Route to Synergistic Magnetic/Conducting Materials, Journal of the American Chemical Society 132(5) 1532-1544, (2010).

[13] L.A. Luo, S.H. Choi, C.D. Frisbie, Probing Hopping Conduction in Conjugated Molecular Wires Connected to Metal Electrodes, Chemistry of Materials 23(3) 631-645, (2011).

[14] D.M. Rowe, Thermoelectrics Handbook: Macro to Nano, CRC Press 2005.

[15] J.P. Heremans, V. Jovovic, E.S. Toberer, A. Saramat, K. Kurosaki, A. Charoenphakdee, S. Yamanaka, G.J. Snyder, Enhancement of Thermoelectric Efficiency in PbTe by Distortion of the Electronic Density of States, Science 321(5888) 554-557, (2008).

[16] A. Weathers, Z.U. Khan, R. Brooke, D. Evans, M.T. Pettes, J.W. Andreasen, X. Crispin, L. Shi, Significant Electronic Thermal Transport in the Conducting Polymer Poly(3,4-ethylenedioxythiophene), Advanced Materials 27(12) 2101-2106, (2015).

[17] J. Liu, X. Wang, D. Li, N.E. Coates, R.A. Segalman, D.G. Cahill, Thermal Conductivity and Elastic Constants of PEDOT:PSS with High Electrical Conductivity, Macromolecules 48(3) (2015) 585-591.
[18] B. Poudel Bed, Q. Hao, Y. Ma, Y. Lan, A. Minnich, High-thermoelectric performance of nanostructured bismuth antimony telluride bulk alloys, SCIENCE 320(5876) (2008) 634-8.
[19] X.A. Yan, B. Poudel, Y. Ma, W.S. Liu, G. Joshi, H. Wang, Y.C. Lan, D.Z. Wang, G. Chen, Z.F. Ren, Experimental Studies on Anisotropic Thermoelectric Properties and Structures of n-Type Bi2Te2.7Se0.3, Nano Lett. 10(9) 3373-3378, (2010).
[20] G. Kanatzidis Mercouri, Advances in thermoelectrics: From single phases to hierarchical nanostructures and back, MRS Bulletin 40(8) 687-694, (2015).
[21] Y. Chen, Y. Zhao, Z. Liang, Solution processed organic thermoelectrics: towards flexible thermoelectric modules, Energy and Environmental Science 8(2) 401-422, (2015).
[22] J.A. Heeger Alan, Semiconducting polymers: the Third Generation, Chemical Society Reviews 39(7) 2354, (2000).
[23] O. Bubnova, Z.U. Khan, H. Wang, S. Braun, D.R. Evans, M. Fabretto, P. Hojati-Talemi, D. Dagnelund, J.B. Arlin, Y.H. Geerts, S. Desbief, D.W. Breiby, J.W. Andreasen, R. Lazzaroni, W.M.M. Chen, I. Zozoulenko, M. Fahlman, P.J. Murphy, M. Berggren, X. Crispin, Semi-metallic polymers (vol 13, pg 190, 2014), Nature Materials 13(6) 662-662, (2014).
[24] G.H. Kim, L. Shao, K. Zhang, K.P. Pipe, Engineered doping of organic semiconductors for enhanced thermoelectric efficiency, Nature Materials 12(8) 719-723, (2013).
[25] B. Russ Boris, M.J. Robb, F.G. Brunetti, P.L. Miller, E.E. Perry, Power factor enhancement in solution-processed organic n-type thermoelectrics through molecular design, Advanced Materials 26(21) 3473, (2014).
[26] G. Gliemann, H. Yersin, SPECTROSCOPIC PROPERTIES OF THE QUASI ONE-DIMENSIONAL TETRACYANOPLATINATE(II) COMPOUNDS, Structure and Bonding 62 87-153, (1985).
[27] J.-L. Zhuang, D. Ar, X.-J. Yu, J.-X. Liu, A. Terfort, Patterned Deposition of Metal-Organic Frameworks onto Plastic, Paper, and Textile Substrates by Inkjet Printing of a Precursor Solution, Advanced Materials 25(33) 4631-4635, (2013).
[28] G.A. Slack, D. Rowe, CRC handbook of thermoelectrics, CRC, Boca Raton, FL 407440 (1995).
[29] P.B. Allen, J.L. Feldman, J. Fabian, F. Wooten, Diffusons, locons and propagons: character of atomic vibrations in amorphous Si, Philosophical Magazine B-Physics of Condensed Matter Statistical Mechanics Electronic Optical and Magnetic Properties 79(11-12) 1715-1731, (1999).
[30] S. Shenogin, A. Bodapati, P. Keblinski, A.J.H. McGaughey, Predicting the thermal conductivity of inorganic and polymeric glasses: The role of anharmonicity, Journal of Applied Physics 105(3) (2009).
[31] J.M. Larkin, A.J.H. McGaughey, Thermal conductivity accumulation in amorphous silica and amorphous silicon, Physical Review B 89(14) (2014).
[32] J.L. Braun, C.H. Baker, A. Giri, M. Elahi, K. Artyushkova, T.E. Beechem, P.M. Norris, Z.C. Leseman, J.T. Gaskins, P.E. Hopkins, Size effects on the thermal conductivity of amorphous silicon thin films, Physical Review B 93(14) (2016).
[33] A. Einstein, Elementary observations on thermal molecular motion in solids, Annalen der Physik 35 679–694, (1911).

[34] D.G. Cahill, S.K. Watson, R.O. Pohl, LOWER LIMIT TO THE THERMAL-CONDUCTIVITY OF DISORDERED CRYSTALS, Physical Review B 46(10) 6131-6140, (1992).
[35] B. Huang, A. McGaughey, M. Kaviany, Thermal conductivity of metal-organic framework 5 (MOF-5): Part I. Molecular dynamics simulations, International Journal of Heat and Mass Transfer 50(3) 393-404, (2007).
[36] X. Wang, C.D. Liman, N.D. Treat, M.L. Chabinyc, D.G. Cahill, Ultralow thermal conductivity of fullerene derivatives, Physical Review B 88(7) (2013).
[37] D.G. Cahill, R.O. Pohl, LATTICE-VIBRATIONS AND HEAT-TRANSPORT IN CRYSTALS AND GLASSES, Annual Review of Physical Chemistry 39 93-121, (1988).
[38] G. Nolas, J. Cohn, G. Slack, Effect of partial void filling on the lattice thermal conductivity of skutterudites, Physical Review B 58(1) 164, (1998).
[39] G.S. Nolas, J. Poon, M. Kanatzidis, Recent developments in bulk thermoelectric materials, MRS Bulletin 31(3) 199-205, (2006).
[40] A. Bentien, M. Christensen, J. Bryan, A. Sanchez, S. Paschen, F. Steglich, G. Stucky, B. Iversen, Thermal conductivity of thermoelectric clathrates, Physical Review B 69(4) 045107, (2004).
[41] A. McGaughey, M. Kaviany, Thermal conductivity decomposition and analysis using molecular dynamics simulations: Part II. Complex silica structures, International Journal of Heat and Mass Transfer 47(8) 1799-1816, (2004).
[42] X. Shi, H. Kong, C.-P. Li, C. Uher, J. Yang, J. Salvador, H. Wang, L. Chen, W. Zhang, Low thermal conductivity and high thermoelectric figure of merit in n-type BaxYbyCo4Sb12 double-filled skutterudites, Applied Physics Letters 92(18) 182101, (2008).
[43] T. Tadano, Y. Gohda, S. Tsuneyuki, Impact of Rattlers on Thermal Conductivity of a Thermoelectric Clathrate: A First-Principles Study, Physical review letters 114(9) 095501, (2015).
[44] W. Qiu, L. Xi, P. Wei, X. Ke, J. Yang, W. Zhang, Part-crystalline part-liquid state and rattling-like thermal damping in materials with chemical-bond hierarchy, Proceedings of the National Academy of Sciences of the United States of America 111(42) 15031-15035, (2014).
[45] K.J. Erickson, F. Leonard, V. Stavila, M.E. Foster, C.D. Spataru, R.E. Jones, B.M. Foley, P.E. Hopkins, M.D. Allendorf, A.A. Talin, Thin Film Thermoelectric Metal-Organic Framework with High Seebeck Coefficient and Low Thermal Conductivity, Advanced Materials 27(22) 3453-3459, (2015).
[46] B.L. Huang, Z. Ni, A. Millward, A.J.H. McGaughey, C. Uher, M. Kaviany, O. Yaghi, Thermal conductivity of a metal-organic framework (MOF-5): Part II. Measurement, Int. J. Heat Mass Transfer 50(3-4) 405-411, (2007).
[47] J.C. Duda, P.E. Hopkins, Y. Shen, M.C. Gupta, Exceptionally Low Thermal Conductivities of Films of the Fullerene Derivative PCBM, Physical Review Letters 110(1) (2013).
[48] J.C. Duda, P.E. Hopkins, Y. Shen, M.C. Gupta, Thermal transport in organic semiconducting polymers, Applied Physics Letters 102(25) (2013).
[49] X. Tang, W. Xie, H. Li, W. Zhao, Q. Zhang, M. Niino, Preparation and thermoelectric transport properties of high-performance p-type Bi2Te3 with layered nanostructure, Applied Physics Letters 90(1) (2007).
[50] X.B. Zhao, X.H. Ji, Y.H. Zhang, T.J. Zhu, J.P. Tu, X.B. Zhang, Bismuth telluride nanotubes and the effects on the thermoelectric properties of nanotube-containing nanocomposites, Applied Physics Letters 86(6) (2005).

DISTRIBUTION

1	MS0359	D. Chavez, LDRD Office	1911
1	MS1415	Carlos Gutiérrez	1874
1	MS9054	Sarah Allendorf	8350
1	MS9161	Christian Mailhiot	8340
1	MS9161	Mark D. Allendorf	8300
1	MS0899	Technical Library	9536 (electronic copy)


Sandia National Laboratories